

Nanocomposite Random Lasers

K. Piperaki, A. Stasinopoulos, D. Anglos, S. H. Anastasiadis, R. N. Das, and
E. P. Giannelis

Foundation for Research & Technology - Hellas (FO.R.T.H.)

Institute of Electronic Structure & Laser (I.E.S.L.)

711 10 Heraklion Crete, Greece

The objective of this project has been to develop new generations of random lasers based on inorganic particle - polymer nanocomposites.

Research on systems described by the general term random lasers has been growing fast in the last few years. In a regular laser cavity, emitted photons reflected by the cavity mirrors travel back and forth through a homogeneous gain medium stimulating the emission of intense coherent radiation, the laser beam. It is highly surprising that similar effects, namely light amplification, can in fact take place in systems exhibiting high degree of disorder such as for example solutions of organic dyes containing scattering particles or even semiconductor powders. While scattering has been considered detrimental in the operation of regular laser systems in the case of random lasers it is the critical condition for providing gain. Apparently recurrent scattering of fluorescence from microcavities defined by two or more particles provides an efficient way of light amplification within the excitation volume. The observed behavior is often described by the term random laser, which points out to the randomness of the system and the fact that the radiation emitted upon pumping exhibits certain characteristics similar to laser action such as spectral and temporal narrowing, threshold gain behavior and, under certain circumstances, laser modes and coherence.

The lasing action in a disordered gain medium is considered to be based on the principle that, in a system with gain and strong scattering centers, the recurrent scattering events (due to multiple scattering) may lead to long light paths within the medium (effectively “trapping” light in a small volume). If the amplification along such light paths exceeds the loss, photon amplification may occur. Such random laser action was first observed in a colloidal solution of scattering particles in the presence of a dye,¹ in polycrystalline films of a semiconductor deposited onto a substrate² as well as in a semiconductor powder film deposited onto a substrate by electrophoresis.³ Moreover, the transition from amplified spontaneous emission to laser action in strong scattering media has been studied⁴ as well as the spatial confinement of the lasing action.⁵ Besides the spectral narrowing, the temporal narrowing of the fluorescence emission was studied by measuring the time-resolved fluorescence signals,⁶ whereas the coherence of the temporally and

¹ N. M. Lawandy, R. M. Balachandran, A. S. L. Gomes, and E. Sauvaln, *Nature* **368**, 436 (1994).

² H. Cao, Y. G. Zhao, H. C. Ong, S. T. Ho, J. Y. Dai, J. Y. Wu, and R. P. H. Chang, *Appl. Phys. Lett.* **73**, 3656 (1998).

³ H. Cao, Y. G. Zhao, S. T. Ho, E. W. Seelig, Q. H. Wang, and R. P. H. Chang, *Phys. Rev. Lett.* **82**, 2278 (1999).

⁴ H. Cao, J. Y. Xu, S.-H. Chang, and S. T. Ho, *Phys. Rev. E* **61**, 1985 (2000).

⁵ H. Cao, J. Y. Xu, D. Z. Zhang, S.-H. Chang, S. T. Ho, E. W. Seelig, X. Liu, and R. P. H. Chang, *Phys. Rev. Lett.* **84**, 5584 (2000).

⁶ G. Zacharakis, G. Heliotis, G. Filippidis, D. Anglos, and T. G. Papazoglou, *Appl. Optics* **38**, 6087 (2000).

REPORT DOCUMENTATION PAGE			Form Approved OMB No. 0704-0188	
Public reporting burden for this collection of information is estimated to average 1 hour per response, including the time for reviewing instructions, searching existing data sources, gathering and maintaining the data needed, and completing and reviewing the collection of information. Send comments regarding this burden estimate or any other aspect of this collection of information, including suggestions for reducing this burden to Washington Headquarters Services, Directorate for Information Operations and Reports, 1215 Jefferson Davis Highway, Suite 1204, Arlington, VA 22202-4302, and to the Office of Management and Budget, Paperwork Reduction Project (0704-0188), Washington, DC 20503.				
1. AGENCY USE ONLY (Leave blank)		2. REPORT DATE 26 Nov ember 2002		3. REPORT TYPE AND DATES COVERED Final Report
4. TITLE AND SUBTITLE Nanocomposite Random Lasers			5. FUNDING NUMBERS F61775-00-WE	
6. AUTHOR(S) Dr Steponas Giannelis and Dr Spiros Anastasiadis				
7. PERFORMING ORGANIZATION NAME(S) AND ADDRESS(ES) FORTH, Foundation for Research & Technology--Hellas PO Box 1527 711 10 Heraklion, Crete Heraklion 711 10 Greece			8. PERFORMING ORGANIZATION REPORT NUMBER N/A	
9. SPONSORING/MONITORING AGENCY NAME(S) AND ADDRESS(ES) EOARD PSC 802 BOX 14 FPO 09499-0200			10. SPONSORING/MONITORING AGENCY REPORT NUMBER SPC 00-4070	
11. SUPPLEMENTARY NOTES				
12a. DISTRIBUTION/AVAILABILITY STATEMENT Approved for public release; distribution is unlimited.			12b. DISTRIBUTION CODE A	
13. ABSTRACT (Maximum 200 words) This report results from a contract tasking FORTH, Foundation for Research & Technology--Hellas as follows: The contractor will synthesize polymer nanocomposite materials and will investigate their properties appropriate to developing a new generation of flexible lasers. The contractor will develop composites by: incorporating semiconductor nanoparticles (ZnO, ZnS, ZnSe, and others) into inert polymer matrices; by incorporating high refractive index nanoparticles (TiO2, BaTiO3, and others) into fluorescent conjugated polymers; and by synthesizing nanocomposites using commercially available nonlinear polymers. The contractor will deposit synthesized nanocomposites onto various surfaces and will characterize their dispersion characteristics, viscoelastic properties, and optical properties for lasing.				
14. SUBJECT TERMS EOARD, Chemistry, lasers and laser engineering, Composites			15. NUMBER OF PAGES 15	
			16. PRICE CODE N/A	
17. SECURITY CLASSIFICATION OF REPORT UNCLASSIFIED	18. SECURITY CLASSIFICATION OF THIS PAGE UNCLASSIFIED	19. SECURITY CLASSIFICATION OF ABSTRACT UNCLASSIFIED	20. LIMITATION OF ABSTRACT UL	

spectrally narrowed emission was studied by carrying out experiments of photon counting statistics.⁷ Recent theories attempt to model the lasing phenomenon in a disordered system.⁸

Our approach within this project involves the investigation of three types of systems:

I) Semiconductor Particles in an Inert Polymer Matrix

ZnO particles were embedded in a polymer such as epoxy, polyimide, or polydimethylsiloxane. The semiconductor particles constitute the active centers providing both gain and scattering.

II) Scattering Particles in an Optically Active Polymer Matrix

In this system, particles with high refractive index including ZnO, TiO₂ and BaTiO₃ will be introduced into a highly fluorescent conjugated polymer such as poly(2-methoxy,5-(2'-ethyl-hexyloxy)-1,4-phenylene-vinylene), MEH-PPV, which will provide the gain medium.

III) Laser Dye and Scattering Particles in an Inert Polymer Matrix

A laser dye such as rhodamine or coumarine would provide the gain, while TiO₂ or BaTiO₃ were the scattering centers. This more conventional system would be compared and contrasted with the ones described above.

In previous reports we demonstrated the lasing action in organic/inorganic nanocomposites consisting of pristine and surface-modified ZnO nanoparticles (average size: 125 nm) dispersed in an optically inert polymer matrix (epoxy or polydimethylsiloxane),⁹ system type I, and we discussed the differences with the more traditional system type III. The ZnO particles provide both the gain and the strong scattering power, which leads to light trapping due to multiple scattering, while the polymer matrix offers ease of material fabrication and processability in view of potential applications. Excitation of the nanohybrids by a laser pulse, with duration shorter than the ZnO photoluminescence lifetime, leads to a dramatic increase in the emitted light intensity, accompanied by a significant spectral and temporal narrowing above a certain pump energy density threshold. Critical laser and materials parameters, which influence the observed laser-like behavior, have been investigated in a series of nanocomposites.¹⁰ Moreover, lasing action in the more classical system (organic dye plus scattering particles in an inert polymer matrix) has been presented in earlier reports and was discussed in relation to the ZnO/polymer system.

In the present report, we present our investigation on the systems type II, i.e. nanocomposites containing poly(2-methoxy,5-(2'-ethyl-hexyloxy)-1,4-phenylene-vinylene), MEH-PPV, as the active medium and ZnO particles (which, however, act only as the scatterers in this system). It is this area that was the focus of the project within the current phase. MEH-PPV is a highly luminescent polymer, transparent or scattering solutions of which have been shown to exhibit laser characteristics upon pumping.¹¹

⁷ G. Zacharakis, N. Papadogiannis, G. Filippidis, and T. G. Papazoglou, *Optics Lett.* **25**, 923 (2000).

⁸ X. Jiang, and C. M. Soukoulis, *Phys. Rev. Lett.* **85**, 70 (2000).

⁹ E. P. Giannelis, A. Stasinopoulos, M. Psyllaki, G. Zacharakis, R. Das, D. Anglos, S. H. Anastasiadis and R.A. Vaia, In "*Hybrid Organic-Inorganic Materials*", R. M. Laine, S. Yang, C. Sanchez, and C. J. Brinker, Eds., Materials Research Society Symposium Proceedings, Vol. **726**, p. Q2.2.1-Q2.1.9, Pittsburgh, PA, 2002.

¹⁰ D. Anglos, A. Stassinopoulos, R.N. Das, G. Zacharakis, M. Psyllaki, R. Jakubiak, S. H. Anastasiadis, R. A. Vaia, and E. P. Giannelis, submitted to *Advanced Materials* (2002).

¹¹ G. J. Denton, N. Tessler, M. A. Stevens, R. H. Friend, *Advanced Materials* **9**, 547 (1997); F. Hide, B. J. Schwartz, M. A. Diaz-Garcia, A. J. Heeger, *Chem. Phys. Lett.* **256**, 424 (1996).

Initial tests included studies of neat MEH-PPV films, which upon excitation at 532nm exhibited the usual fluorescence emission but no tendency for narrowing. This was attributed to intermolecular quenching of the MEH-PPV emission resulting from its very high concentration. The presence or absence of scattering particles had no effect.

On the basis of these findings we fabricated samples composed of mixtures of MEH-PPV with polystyrene (PS) at various concentrations of PPV, which also contained varying amounts of ZnO (or TiO₂) scattering particles. Indeed, in most cases, increasing the pump energy density resulted in a gradual spectral narrowing of the emitted fluorescence. In all measurements the second harmonic of a Nd:YAG laser with wavelength 532 nm and pulse duration 5 ns, was used. It is noted that ZnO is not excited at this wavelength.¹²

Initial Experiments

The early investigation on these systems (MEH-PPV / PS / scatterers) concentrated on the possibility of observing laser-like emission from these systems. Two systems were investigated whose characteristics are shown in Table 1 (the first two systems). These have been presented in the previous report but they are also presented herein for completeness.

Table 1: Sample Characteristics

Sample Code	MEH-PPV %(w/w)	ZnO (125±25nm) %(w/w)	TiO ₂ (400nm) %(w/w)
PPV-1.5-2ZnO	1.5	2	-
PPV-1.5-2TiO ₂	1.5	-	2
PPV-0.25-2ZnO	0.25	2	-
PPV-2-2ZnO	2	2	-
PPV-4-2ZnO	4	2	-
PPV-2-4ZnO	2	4	-
PPV-2-8ZnO	2	8	-
PPV-0.25	0.25	-	-
PPV-8	8	-	-

Figure 1 shows indicative spectra (focusing on the main emission band at ~610 nm) at low and high pump energy density from a sample of PPV-PS/ZnO excited at 532nm, showing the spectral narrowing observed. When pumped at low energy, the spectrum is very broad (full-width-at-half-maximum, FWHM, of about 45 nm), whereas when pumped at high energies the spectrum becomes narrow (FWHM about 10 nm).

A significant difference between the behavior of the present system and that of the ZnO/polymer system is the absence of a clear indication of a threshold-like behavior in the present case, especially in the behavior of the spectral width versus pump energy. Figure 2 shows the dependence of the fluorescence emission intensity on the pump energy density for a PPV-PS/ZnO (PPV: 1.5% w/w, ZnO: 2%w/w) specimen with 0.16 cm² focusing spot. A

¹² The possibility of directly pumping ZnO using the UV output of the Nd:YAG laser (355nm) was also investigated in order to exploit the chromophore properties of ZnO in combination to its scattering action in a manner similar to that followed in the part I of this project where ZnO/PDMS systems were studied. However, it was not possible to obtain strong emission from the ZnO particles most probably because of the high absorption coefficient of MEH-PPV in the UV (measured independently both in solution and for thin MEH-PPV films), which prevents effective excitation of ZnO and also absorbs most of the ZnO luminescence.

weak deviation from the almost linear dependence is observed in contrast to the clear gain behavior observed in the ZnO/polymer and in the organic dye/scatterers/polymer systems. Figure 3 shows the dependence of the respective FWHM on the pump energy density. Although spectral narrowing is observed, this appears to take place in a rather gradual fashion instead of the abrupt transition from wide to narrow common to the ZnO/polymer and in the organic dye/scatterers/polymer systems.

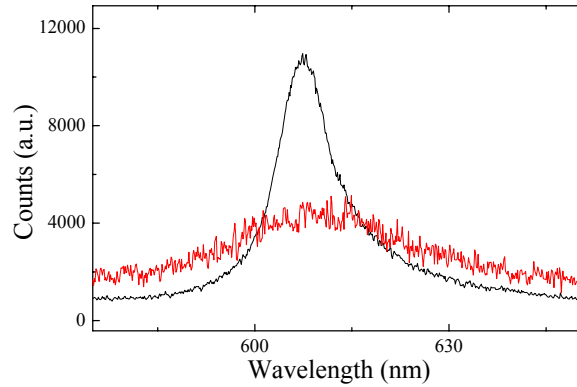


Figure 1. Emission spectra of PPV-PS/ZnO (PPV: 1.5% w/w, ZnO: 2%w/w) following excitation at 532nm. The illuminated spot size is 0.16 cm^2 . The low intensity spectrum has been scaled up by a factor of 10.

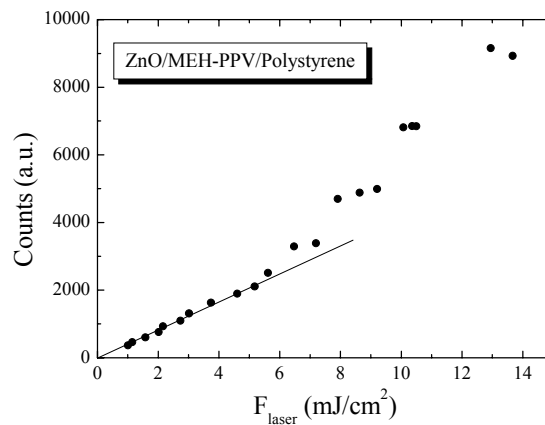


Figure 2. Fluorescence intensity as a function of the pump energy density of PPV-PS/ZnO (PPV: 1.5% w/w, ZnO: 2%w/w) following excitation at 532nm and 0.16 cm^2 spot size.

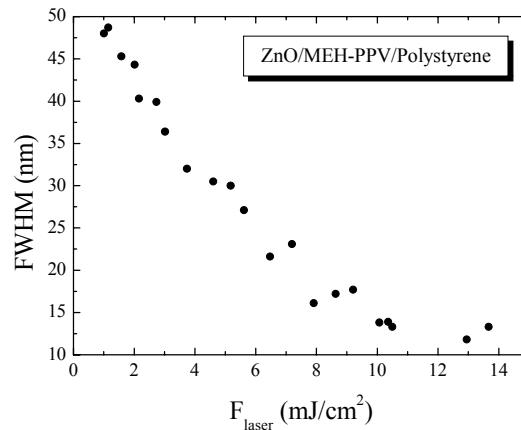


Figure 3. Emission peak FWHM as a function of the pump energy density of PPV-PS/ZnO (PPV: 1.5% w/w, ZnO: 2%w/w) following excitation at 532nm and 0.16 cm^2 spot size.

A similar behavior is observed in the case of the PPV-PS/TiO₂ system. Figure 4 shows the dependence of the fluorescence emission intensity on the pump energy density for a PPV-PS/ TiO₂ (PPV: 1.5% w/w, TiO₂: 2%w/w) specimen with 0.008 cm² focusing spot. Again, a weak deviation from the almost linear dependence is observed. Figure 5 shows the dependence of the respective FWHM on the pump energy density. Once more, although spectral narrowing is observed, this takes place in a gradual fashion without any indication of a threshold behavior. We anticipate that this is due to the very low volume fraction of strong scatterers in both systems and experiments were planned with increasing fraction of scattering particles.

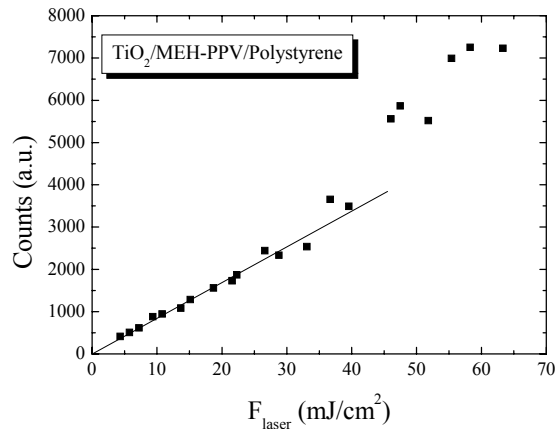


Figure 4. Fluorescence intensity as a function of the pump energy density of PPV-PS/TiO₂ (PPV: 1.5% w/w, TiO₂: 2%w/w) following excitation at 532nm and 0.008 cm² spot size.

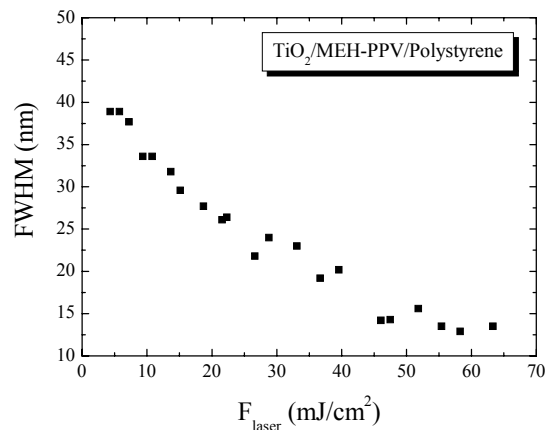


Figure 5. Emission peak FWHM as a function of the pump energy density of PPV-PS/TiO₂ (PPV: 1.5% w/w, TiO₂: 2%w/w) following excitation at 532nm and 0.008 cm² spot size.

It is noted that the focusing spot for Figures 4 and 5 is 20 times less than in Figures 2 and 3. As we had shown in earlier reports the focusing spot is a parameter that influences significantly the threshold values; when the irradiation surface area decreases the observed threshold for lasing increases.⁹

In parallel, the stability of the emission behavior was investigated and is demonstrated in Figures 6 and 7. At low excitation energy (Figure 6) a series of successive weak emission spectra are recorded while at high energy (Figure 7) narrow spectra are observed with good stability, as well. We had shown before that the relation of the laser pulse width with the emission lifetime plays a crucial role in the stability of the phenomenon.⁹

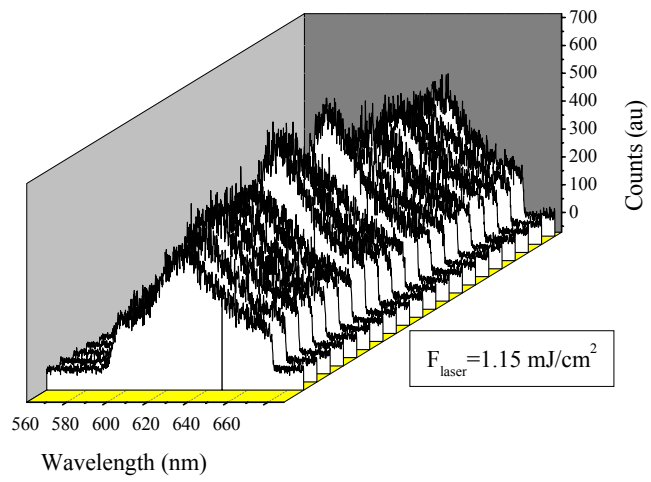


Figure 6. Emission spectra following 20 successive pulses at a low incident energy density. Sample PPV-PS/ZnO (PPV: 1.5% w/w, ZnO: 2%w/w)

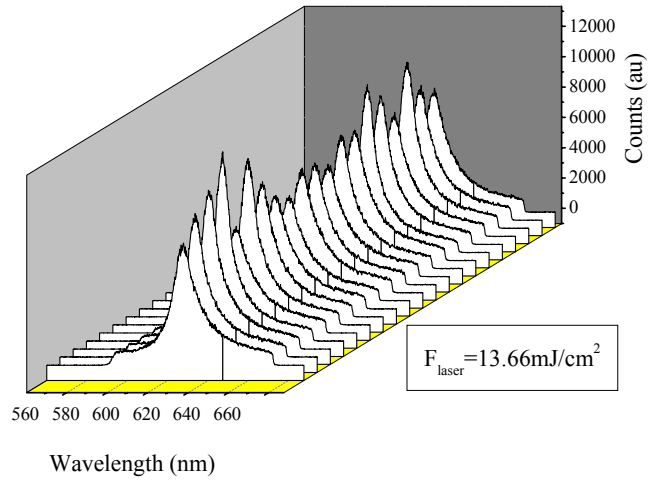


Figure 7. Emission spectra following 20 successive pulses at a high incident energy density. Sample PPV-PS/ZnO (PPV: 1.5% w/w, ZnO: 2%w/w)

Systematic Investigation

Following the initial measurements and the observation of spectral narrowing, a more systematic series of specimens (MEH-PPV / PS / scatterers) was prepared with varying amounts of MEH-PPV and/or ZnO particles. The characteristics of the systems investigated are also shown in Table 1.

Figure 8 shows a series of emission spectra from low to high pump energy density (0.01 to 4.41 mJ/pulse) from a sample of MEH-PPV/PS/ZnO (MEH-PPV: 0.25% w/w, ZnO: 2% w/w) excited at 532nm with 0.0351 cm² focusing spot. For this sample with very low content of the fluorescent polymer neither a significant increase of the intensity nor any important spectral narrowing is observed.

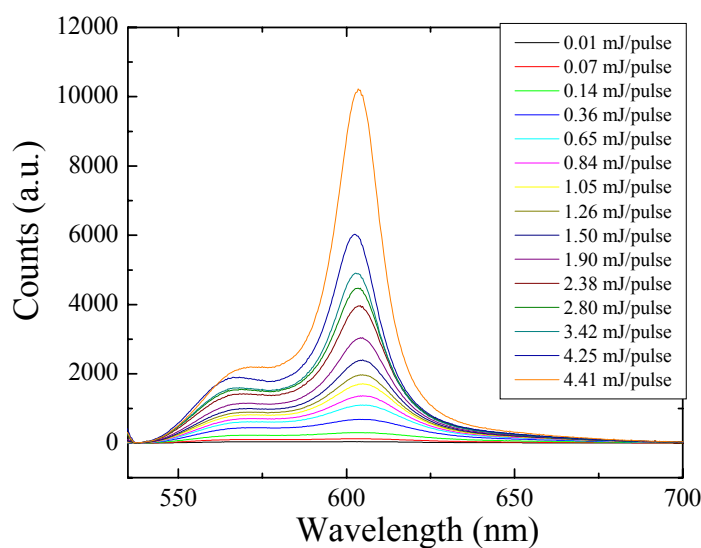


Figure 8. Emission spectra of MEH-PPV/PS/ZnO (MEH-PPV: 0.25% w/w, ZnO: 2% w/w at) at varying (0.01-4.41 mJ/pulse) pump energy density following excitation at 532 nm. The illuminated spot size is 0.0351 cm².

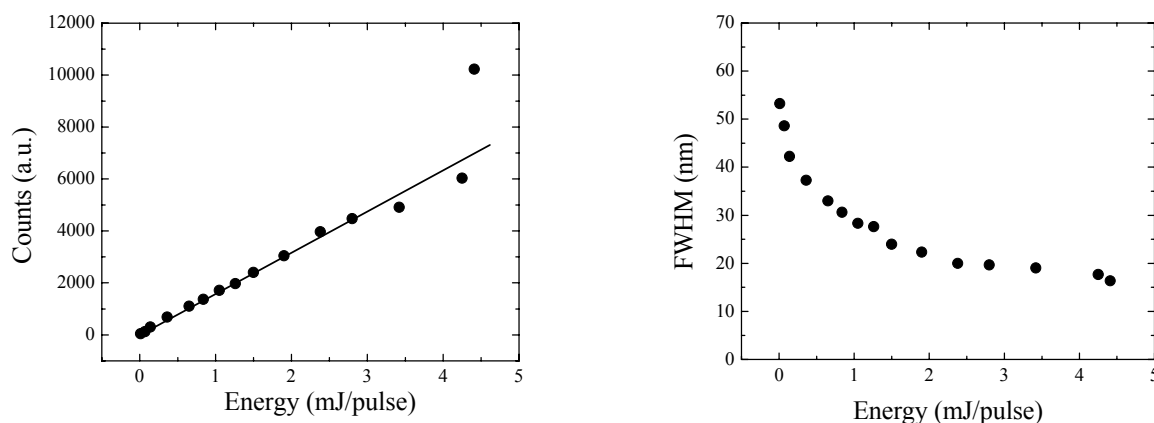


Figure 9. Fluorescence intensity and emission peak FWHM as a function of the pump energy density of MEH-PPV/PS/ZnO (MEH-PPV: 0.25% w/w, ZnO: 2% w/w) following excitation at 532 nm and 0.0351 cm² spot size

Figure 9 shows the dependence of the fluorescence emission intensity and the emission peak full-width-at-half-maximum, FWHM,¹³ on the pump energy density for the same specimen. The emission intensity does not deviate from the linear dependence on the pump energy whereas a gradual spectral narrowing is observed.

Figure 10 shows indicative spectra at four different pump energy densities from a sample of MEH-PPV/PS/ZnO (MEH-PPV: 2% w/w, ZnO: 2% w/w) excited at 532nm with 0.0351 cm² focusing spot, showing both the significant increase of the intensity (note the differences in the y-axes) and the spectral narrowing observed. When pumped at low energy, the spectrum is very broad and possesses low intensity, whereas when pumped at high energies the spectrum becomes narrow and of high intensity.

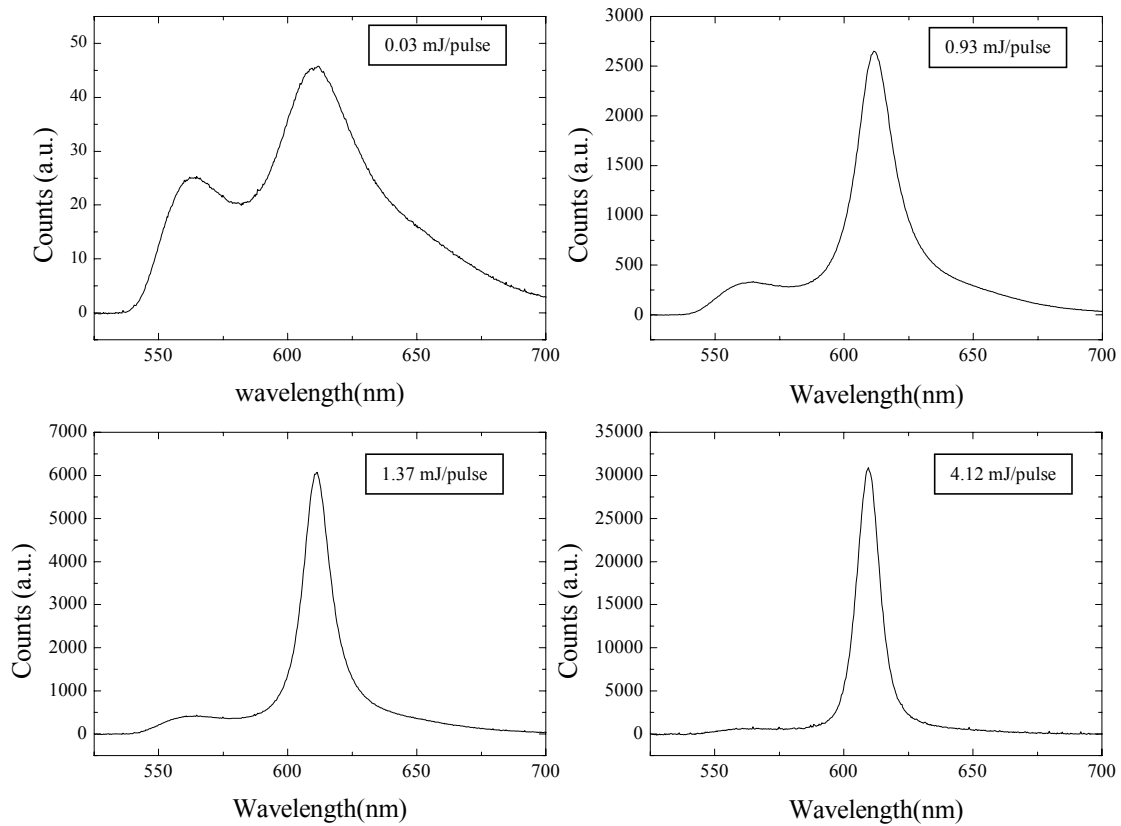


Figure 10. Emission spectra of MEH-PPV/PS/ZnO (MEH-PPV: 2% w/w, ZnO: 2% w/w) at four different pump energy densities following excitation at 532 nm. The illuminated spot size is 0.0351 cm².

Figure 11 shows the dependence of the fluorescence emission intensity and the emission peak full-width-at-half-maximum, FWHM, on the pump energy density for the same specimen. The deviation from the linear dependence of the emission intensity on the pump energy is evident as is the gradual spectral narrowing as pumping energy increases. It is interesting that it appears that the FWHM of the spectra attain a more-or-less constant value for pumping energies higher than the threshold. Moreover, the wavelength of the

¹³ FWHM values were calculated by doubling the values, which are obtained subtracting the wavelengths at which the emission spectra show maximum intensities from the wavelengths on the red sides at which the intensities are half of the corresponding peak values.

emission maximum as a function of pump energy density shifts by only about 2 nm and is not further discussed herein.

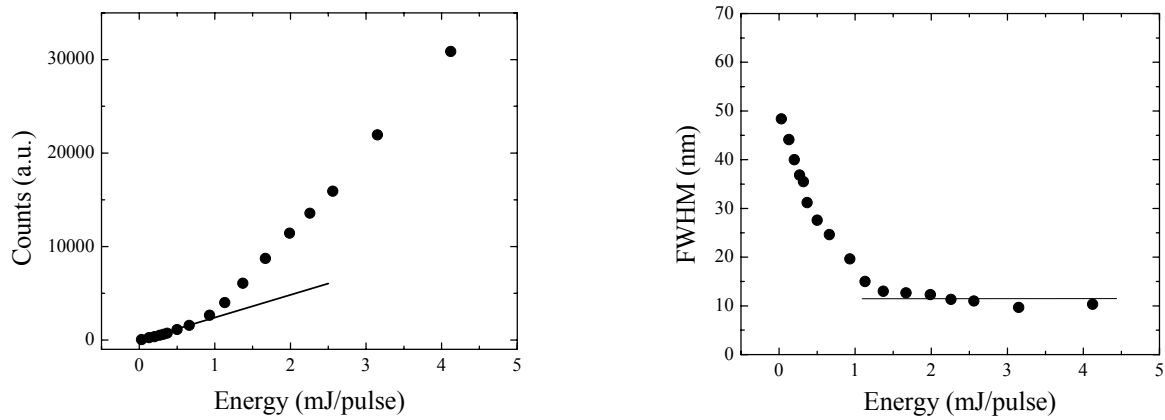


Figure 11. Fluorescence intensity and emission peak FWHM as a function of the pump energy density of MEH-PPV/PS/ZnO (MEH-PPV: 2% w/w, ZnO: 2% w/w) following excitation at 532 nm and 0.0351 cm^2 spot size

Figure 12 shows indicative spectra at low and high pump energy density from a sample of MEH-PPV/PS/ZnO with higher concentration of MEH-PPV (MEH-PPV: 4% w/w, ZnO: 2% w/w). The specimen is excited at 532nm with 0.0351 cm^2 focusing spot. Figure 13 shows the dependence of the fluorescence emission intensity and the emission peak FWHM on the pump energy density.

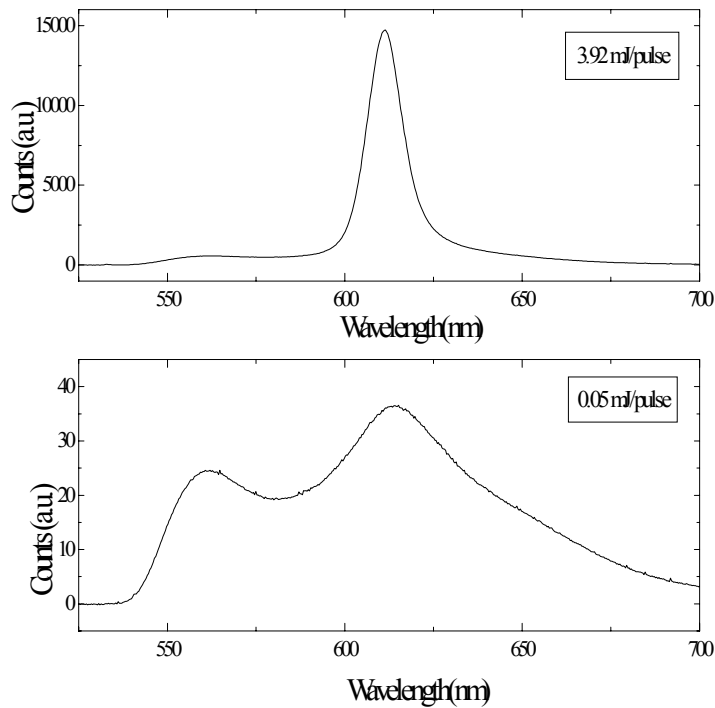


Figure 12. Emission spectra of MEH-PPV/PS/ZnO (MEH-PPV: 4% w/w, ZnO: 2% w/w) at low (0.05 mJ/pulse) and high (3.92 mJ/pulse) pump energy density following excitation at 532 nm. The illuminated spot size is 0.0351 cm^2 .

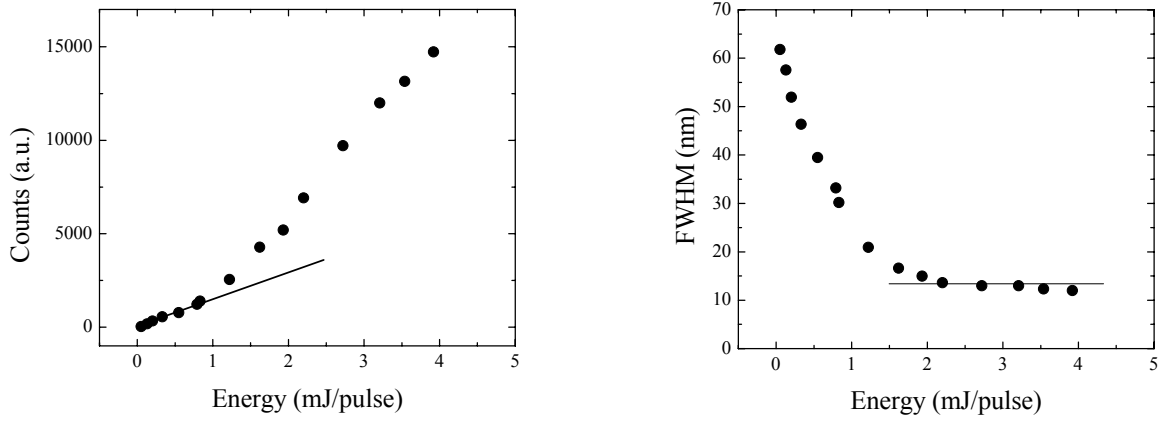


Figure 13. Fluorescence intensity and emission peak FWHM as a function of the pump energy density of MEH-PPV/PS/ZnO (MEH-PPV: 4% w/w, ZnO: 2% w/w) following excitation at 532 nm and 0.0351 cm^2 spot size

Figure 14 compares the behavior of the fluorescence emission intensity and the emission peak FWHM data and their dependence on the pump energy density for the series of MEH-PPV/PS/ZnO specimens with 2 %w/w ZnO and varying amounts of MEH-PPV. It is evident that the deviation from the linear dependence in the intensity plot (i.e., the value of the threshold) depends on the MEH-PPV concentration in a complicated manner: it decreases when going from the 0.25% to 2% whereas it apparently increases again with higher PPV amounts (the same observation holds when the FWHM is considered). This may be related to the possibility of fluorescence quenching at high MEH-PPV concentrations.

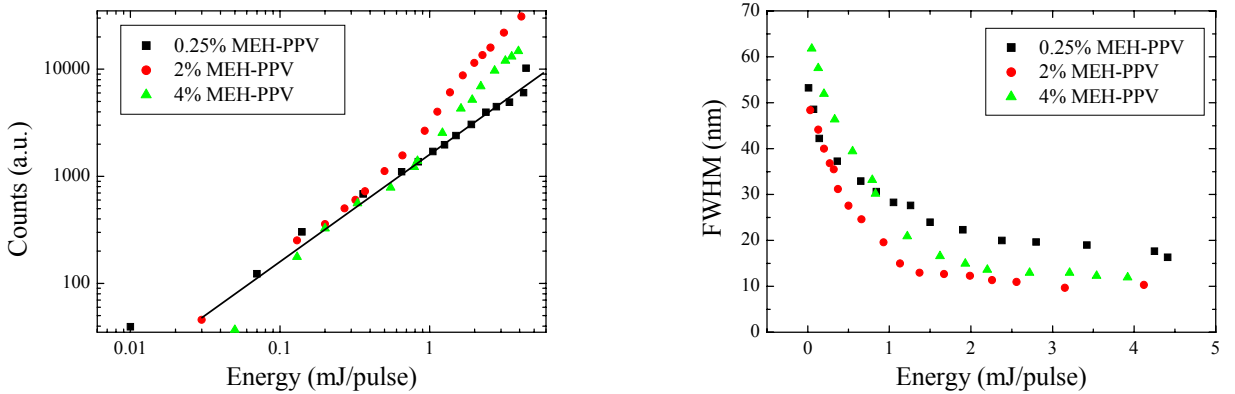


Figure 14. Fluorescence intensity and emission peak FWHM as a function of the pump energy density of MEH-PPV/PS/ZnO (MEH-PPV: 0.25, 2 and 4% w/w, ZnO: 2% w/w) following excitation at 532 nm and 0.0351 cm^2 spot size. The solid line denotes slope 1.

Figure 15 shows indicative spectra at low and high pump energy density from a sample of MEH-PPV/PS/ZnO with a higher concentration of ZnO particles (MEH-PPV: 2% w/w, ZnO: 4% w/w), which was excited at 532nm with 0.0351 cm^2 focusing spot. Moreover, Figure 16 shows the dependence of the fluorescence emission intensity and the emission peak FWHM on the pump energy density.

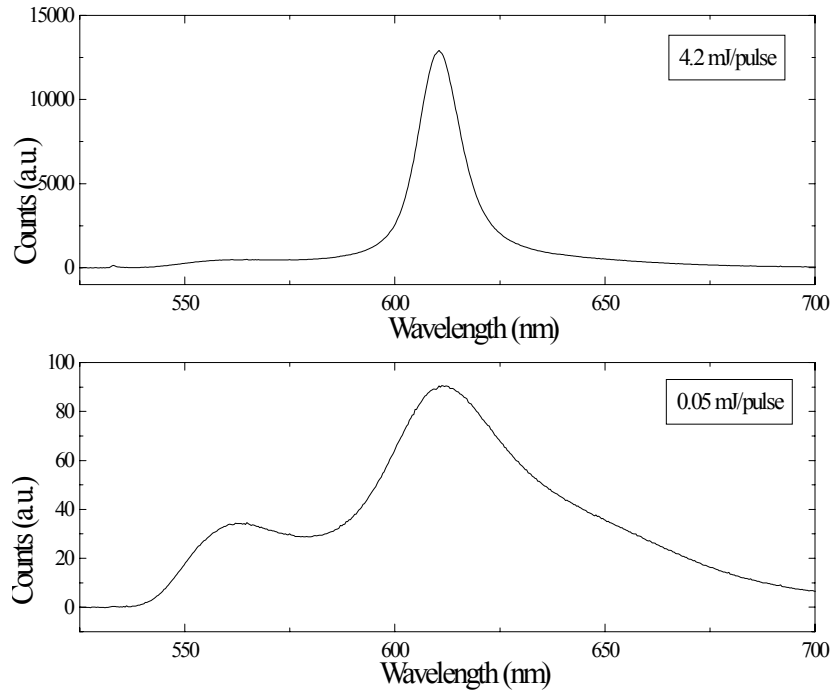


Figure 15. Emission spectra of MEH-PPV/PS/ZnO (MEH-PPV: 2% w/w, ZnO: 4% w/w) at low (0.05 mJ/pulse) and high (4.2 mJ/pulse) pump energy density following excitation at 532 nm. The illuminated spot size is 0.0351 cm^2 .

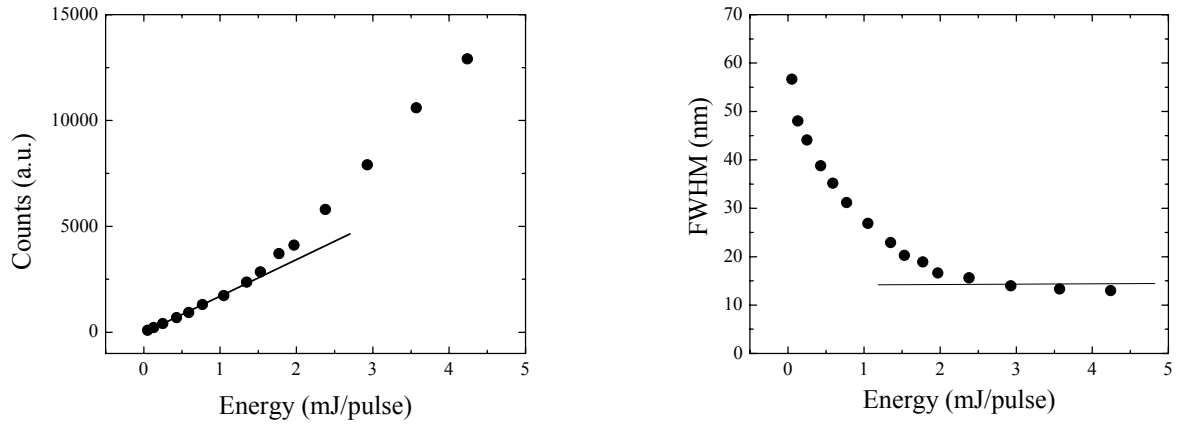


Figure 16. Fluorescence intensity and emission peak FWHM as a function of the pump energy density of MEH-PPV/PS/ZnO (MEH-PPV: 2% w/w, ZnO: 4% w/w) following excitation at 532 nm and 0.0351 cm^2 spot size

Figure 17 shows indicative spectra at low and high pump energy density from a sample of MEH-PPV/PS/ZnO with an even higher concentration of ZnO scattering particles (MEH-PPV: 2% w/w, ZnO: 8% w/w), which was excited at 532nm with 0.0351 cm^2 focusing spot.

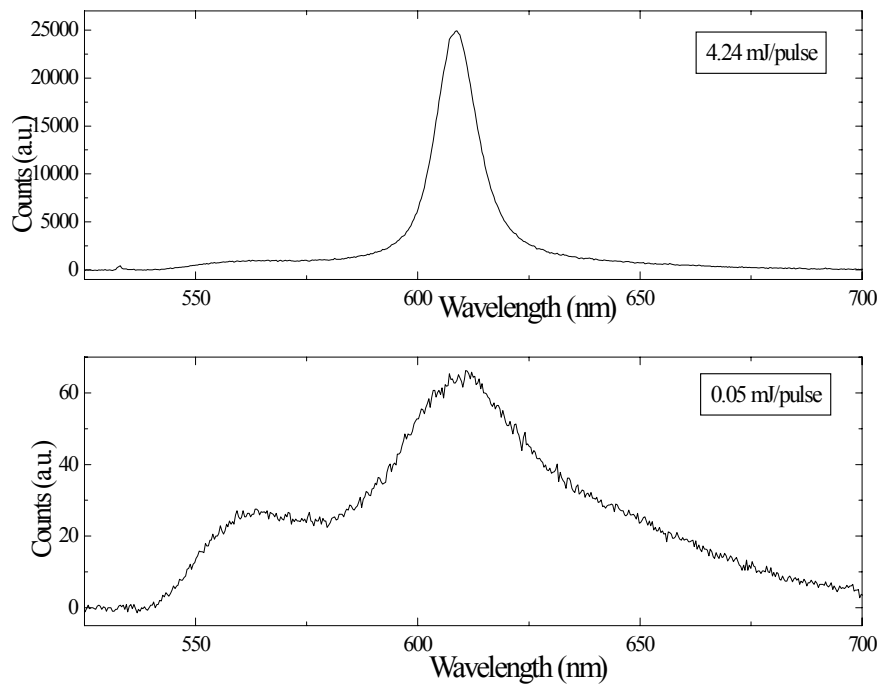


Figure 17. Emission spectra of MEH-PPV/PS/ZnO (MEH-PPV: 2% w/w, ZnO: 8% w/w) at low (0.05 mJ/pulse) and high (4.24 mJ/pulse) pump energy density following excitation at 532 nm. The illuminated spot size is 0.0351 cm^2 .

Figure 18 shows the dependence of the fluorescence emission intensity and the emission peak FWHM on the pump energy density for the same specimen.

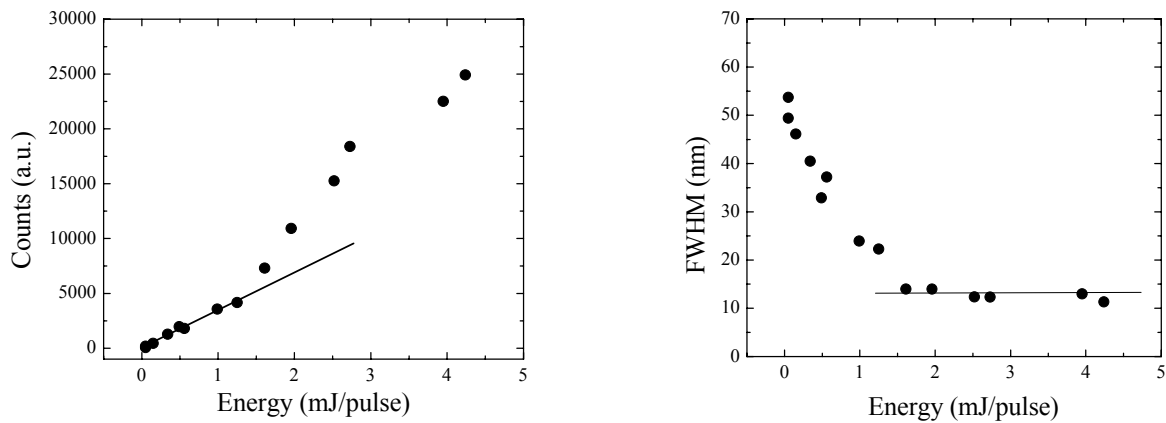


Figure 18. Fluorescence intensity and emission peak FWHM as a function of the pump energy density of MEH-PPV/PS/ZnO (MEH-PPV: 2% w/w, ZnO: 8% w/w) following excitation at 532 nm and 0.0351 cm^2 spot size

Figure 19 compares the behavior of the fluorescence emission intensity and the emission peak FWHM data and their dependence on the pump energy density for the series of MEH-PPV/PS/ZnO specimens with 2 %w/w MEH-PPV and varying amounts of ZnO. It is

evident that the deviation from the linear dependence in the intensity plot (i.e., the value of the threshold) depends on the ZnO concentration in a complicated manner. The same holds for the FWHM. The FWHM attains its low value at much lower pump energies for the 2% w/w ZnO than for 4% or 8% whereas the threshold (estimated from the deviation from the linear dependence in the intensity plot) increases when going from the 2% to 4% whereas it apparently decreases again with higher ZnO amounts. This is different from what was observed for ZnO/PDMS systems⁹ most probably due to miscibility problems in the present MEH-PPV/PS/ZnO systems.

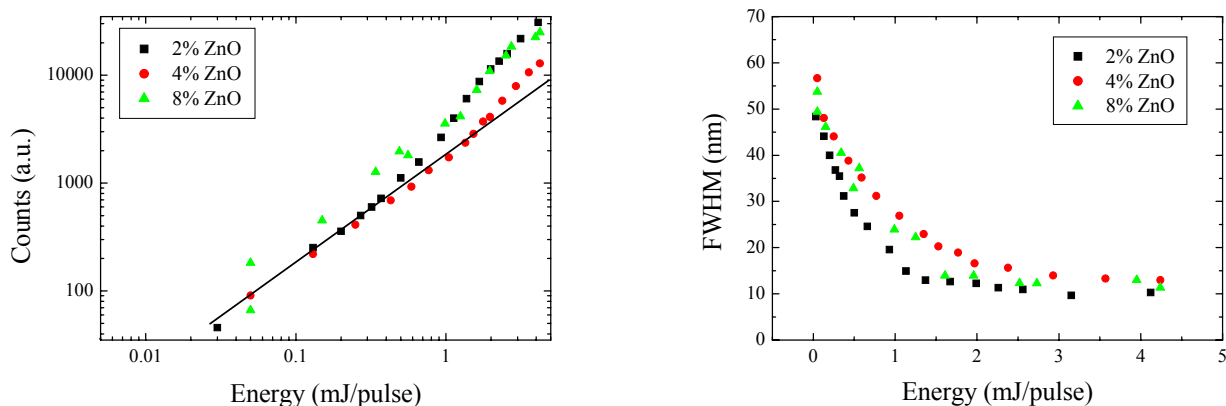


Figure 19. Fluorescence intensity and emission peak FWHM as a function of the pump energy density of MEH-PPV/PS/ZnO (MEH-PPV: 2% w/w, ZnO: 2, 4, and 8% w/w) following excitation at 532 nm and 0.0351 cm^2 spot size. The solid line denotes slope 1.

Binary Systems

Finally, we would like to present the behavior of MEH-PPV/PS blends in the absence of scattering particles in order to investigate (a) the “background” of emission over which the presence of the scattering particles contribute and (b) to study whether one can take advantage of the immiscibility of MEH-PPV/PS (that leads to strongly scattering films) and discuss the possibility of lasing even in the absence of inorganic scattering particles. Two MEH-PPV concentrations were investigated 0.25 and 8% w/w.

Figure 20 shows a series of emission spectra from low to high pump energy density from a MEH-PPV/PS sample with 0.25% w/w PPV excited at 532nm with 0.0351 cm^2 focusing spot, whereas Figure 21 shows the dependence of the fluorescence emission intensity and the emission peak FWHM on the pump energy density for the same specimen. It is evident that the spectra do not show any significant change in the spectral width whereas the intensity exhibits a saturation behavior.

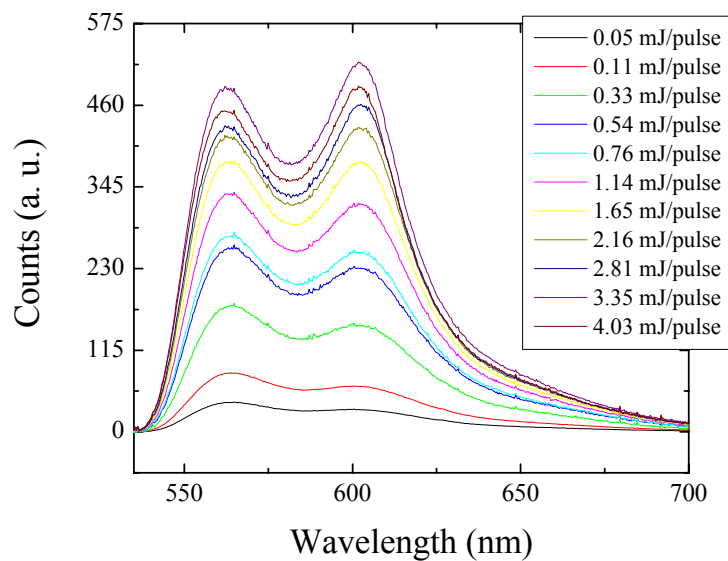


Figure 20. Emission spectra of MEH-PPV/PS (MEH-PPV: 0.25% w/w) at varying (0.05-4.03 mJ/pulse) pump energy following excitation at 532 nm. The illuminated spot size is 0.0351 cm^2 .

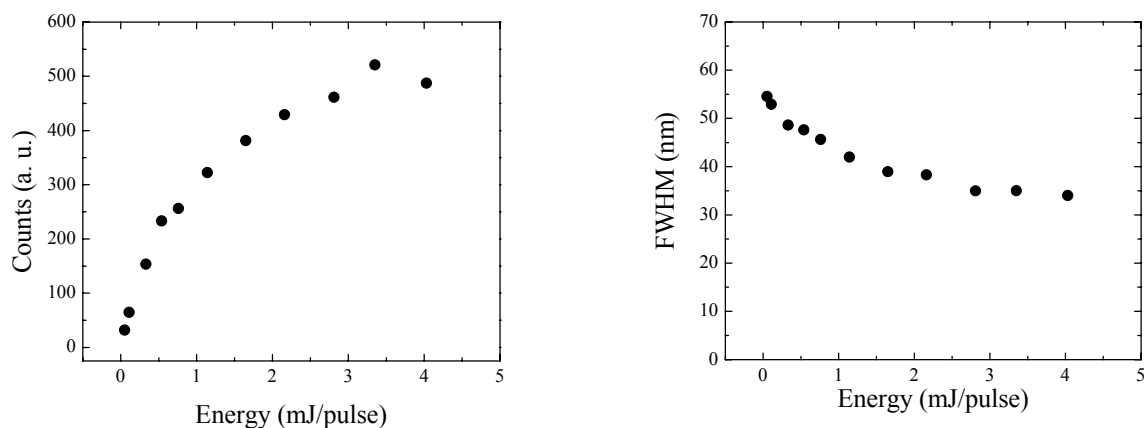


Figure 21. Fluorescence intensity and emission peak FWHM as a function of the pump energy density of MEH-PPV/PS (MEH-PPV: 0.25% w/w, ZnO: 0% w/w) following excitation at 532 nm and 0.0351 cm^2 spot size

Figure 22 shows a series of emission spectra from low to high pump energy density from a MEH-PPV/PS sample with 8% w/w PPV excited at 532nm with 0.0351 cm^2 focusing spot, whereas Figure 23 shows the dependence of the fluorescence emission intensity and the emission peak FWHM on the pump energy density for the same specimen. In this case although the emission intensity does not show any kind of threshold behavior, there is a significant spectral narrowing, which is attributed to the strong scattering of light in the systems due to the phase separated morphology of the MEH-PPV/PS blend at this concentration of PPV.

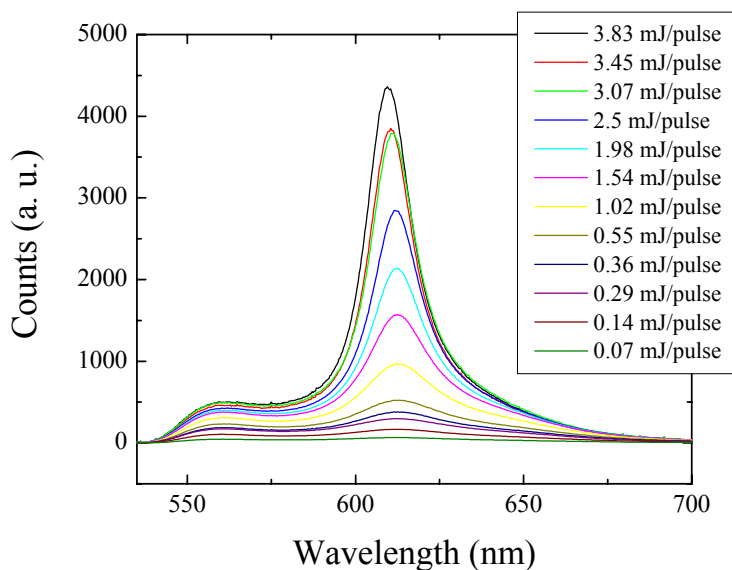


Figure 22. Emission spectra of MEH-PPV/PS (MEH-PPV: 8% w/w) at varying (0.07-3.83 mJ/pulse) pump energy following excitation at 532 nm. The illuminated spot size is 0.0351 cm^2 .

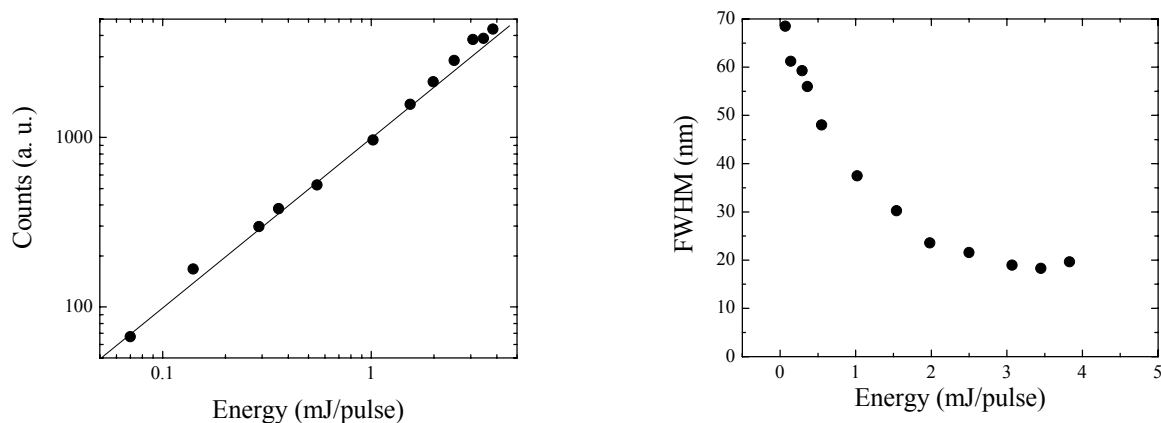


Figure 23. Fluorescence intensity and emission peak FWHM as a function of the pump energy density of MEH-PPV/PS (MEH-PPV: 8% w/w, ZnO: 0% w/w) following excitation at 532 nm and 0.0351 cm^2 spot size. The line denotes slope 1.

In conclusion, the lasing from disordered random media has been investigated for series of MEH-PPV/PS/scatterer hybrids. Key to the observation of spectral narrowing is the use of MEH-PPV in combination with an inert polymer matrix to limit intermolecular quenching effects as well as to reduce cost and improve processability and solubility in common solvents. The effect of the concentration of both the fluorescent polymer and the scattering particles has been investigated.